Proceedings of the 4th International Conference on Applied Physics and Mathematical Modeling
DOI: 10.54254/2753-8818/2026.36117

Numerical Solution of the Schrödinger Equation for Quarkonium Bound States

Ricky Zong

Basis International Park Lane Harbour, Huizhou, China
rzong314@gmail.com

Abstract. Quarkonium, which is a bound state of a heavy quark and its corresponding antiquark, is similar to the hydrogen atom in particle physics, and its spectrum can provide information about the interquark potential of quantum chromodynamics. Numerical solution of the radial Schrödinger equation for charmonium uses the Cornell potential model, which combines the short-range Coulomb term and the linearly rising confining term. Fourth-order Numerov integration is used in combination with inward and outward shooting; they are connected at the classical turning point, and a node labelled energy scan is added to link each root to an excited state. First, this way is validated against the analytical hydrogen spectrum; it has been reproduced to better than one millielectronvolt. Then, based on the experimental measurement of the three lowest S-wave vector states of charmonium, the mass of the charm quark, the strong coupling constant and the confinement coefficient are determined by fitting, and a coarse random search followed by Nelder-Mead simplex refinement is employed for the fit. The converged fit is within 0.01 MeV of the experimental masses, and its root mean square deviation is 0.005 MeV; however, the fitted string tension is lower than its independent value and the fitted coupling is higher than its independent value, which may be due to the omission of spin-spin interaction, relativistic correction and open charm coupled-channel effects. The calculated wave functions have a node structure and their spatial extent grows slowly; it is characteristic of confinement.

Keywords: quarkonium, charmonium, Schrödinger equation, Cornell potential, Numerov method

1. Quarkonium: an overview

1.1. The basic nature of quarkonium

Quarkonium denotes a class of strongly bound, electrically neutral, colour singlet mesons whose constituents are a quark and its own antiquark of the same flavour. The term is normally reserved for the heavy quark bound states in which the constituent masses are large compared to the QCD confinement scale, so that the system admits a non relativistic treatment. The most studied states are charmonium, the bound state of a charm quark and an anti charm quark ($c\bar{c}$), and bottomonium, the bound state of a bottom quark and an anti bottom quark ($b\bar{b}$). A toponium state does not exist as a

© 2026 The Authors. This is an open access article distributed under the terms of the Creative Commons Attribution License 4.0 (https://creativecommons.org/licenses/by/4.0/).

DOI: 10.54254/2753-8818/2026.36117

meaningful bound system, because the top quark decays before a hadron can form [1]; heavy quarkonium is therefore a two flavour phenomenon.

The defining physical feature of quarkonium is that the masses of its constituents are large compared to the energy scale of strong interaction confinement, $\Lambda_{\mathrm{QCD}} \approx 200$ MeV [1]. Because $m_c \approx 1.3$ GeV/c^2 and $m_b \approx 4.2$ GeV/c^2 [1], the constituent quarks move at non relativistic speeds within the bound state. In effect, quarkonium is the closest particle physics analogue of the simplest atomic systems, with the difference that the binding force is the strong interaction rather than electromagnetism.

A characteristic feature of charmonium and bottomonium that distinguishes them from light mesons is that the lowest lying states are narrow resonances. The ground state of charmonium, the J/ψ, has a width of only about 93 keV [1]. The reason is that the J/ψ lies below the threshold for production of a pair of open charm mesons (a $D\bar{D}$ pair), so it cannot decay into hadrons containing charm quarks; the dominant decay proceeds through annihilation of the $c\bar{c}$ pair into three gluons, and since the strong coupling decreases with increasing energy (asymptotic freedom), the total amplitude is suppressed, leading to the long lifetime and narrow width.

1.2. The history of discovery

The experimental discovery of quarkonium is one of the most celebrated episodes in twentieth-century particle physics, the "November Revolution" of 1974. Two independent experiments announced simultaneously the observation of a narrow resonance at a centre of mass energy of approximately 3.1 GeV. At Brookhaven National Laboratory, a group led by Samuel Ting observed an enhancement in the invariant mass spectrum of e^+e^- pairs produced in proton beryllium collisions, and named the new particle the J [2]. At nearly the same time, a group led by Burton Richter at the Stanford Linear Accelerator Center observed an obvious spike in the cross section for $e^+e^- \rightarrow$ hadrons at the same energy, and named the new particle the ψ [3]. The width of the J/ψ resonance, about 93 keV [1], is far smaller than the energy spread of the colliding beams [3]; within a matter of weeks, a broader resonance was observed at 3.686 GeV and was named ψ' (or $\psi(2S)$) [4], quickly understood to be the first radial excitation of the same system.

The interpretation as the bound state of a new heavy quark, the charm quark c, was quickly adopted by the community, completing a second generation in the quark sector and providing the missing ingredient required by the GIM (Glashow Iliopoulos Maiani) mechanism [5]; the bound state $c\bar{c}$ was named charmonium in comparison with positronium. The Upsilon, Y, observed by a group led by Leon Lederman at Fermilab in 1977 as a narrow resonance in the dimuon invariant mass spectrum at approximately 9.46 GeV/c^2 [6], extended the family to bottomonium.

The form of the interquark potential $V(r)$ follows from the two limiting regimes of Quantum Chromodynamics (QCD). At short distances, asymptotic freedom implies that the effective coupling between quarks becomes small, and the gluon exchange interaction should resemble the Coulomb interaction of electrodynamics, with a $-\alpha_s/r$ form (with a colour factor of 4/3 in the colour singlet channel). At large distances, the phenomenon of colour confinement implies that the energy required to separate a quark from an antiquark grows linearly with their separation, as the colour flux between them is squeezed into a tube of approximately constant cross section. Combining the short distance Coulomb like behaviour with the long distance linear confinement leads to the Cornell potential [7-9],

$$V(r) = -\frac{4}{3}\frac{\alpha_s}{r} + br \tag{1}$$

DOI: 10.54254/2753-8818/2026.36117

where α_s is a dimensionless coupling constant and b is a parameter with units of energy per length, often referred to as the string tension.

A piece of evidence for the linearly rising long distance behaviour comes directly from the spacing of the charmonium energy levels. Unlike hydrogen, where energy levels scale as $-1/n^2$ and converge to a finite ionization limit, the charmonium levels show a much more uniform spacing, consistent with the energy spectrum of a linear potential well rather than a Coulomb potential. Numerical solution of the Schrödinger equation with the Cornell potential, as discussed in detail in Section 4, is precisely what is required to make this quantitative.

2. The Schrödinger equation

2.1. The basic equations

The Schrödinger equation is the cornerstone of non relativistic quantum mechanics, the linear partial differential equation whose solutions encode the bound states, scattering states, energy levels, and time evolution of a quantum system [10, 11].

For potentials independent of time, $V = V(\mathrm{r})$, the equation admits separable stationary solutions in which the spatial wave function $\psi(\mathrm{r})$ satisfies the time independent Schrödinger equation,

$$[-\frac{\hbar^2}{2m}\nabla^2 + V(r)]\psi(r) = E\psi(r) \tag{2}$$

a stationary eigenvalue equation for the Hamiltonian. The energy E enters as the eigenvalue, and for potentials that bind the particle the spectrum of allowed energies is discrete. Boundary conditions—typically the requirement that ψ be normalizable, $\int|\psi|^2 d^3r < \infty$—are responsible for the quantization of the energy: only special values of E admit physically acceptable solutions.

2.2. The hydrogen atom: analytic solution

The hydrogen atom is, by common consensus, the single most important exactly solvable problem in three dimensional quantum mechanics. It is the prototype for any system in which a particle moves under a central force, and its solution by separation of variables in spherical coordinates provides the template for the radial problem encountered later in the quarkonium analysis.

For an electron of mass m moving in the Coulomb field of a nucleus of charge Ze, the potential depends only on $r = |\mathrm{r}|$, so the equation admits separable solutions of the form $\psi(\mathrm{r}) = R(r)Y_{\ell,m}(\theta, \varphi)$, where $Y_{\ell,m}$ is a spherical harmonic, an eigenfunction of the orbital angular momentum operators. The mass appearing here should strictly be the reduced mass μ, but the proton to electron mass ratio is sufficiently large that $\mu \approx m_e$ is an excellent approximation for hydrogen. The radial function $R(r)$ then satisfies the radial Schrödinger equation,

$$-\frac{\hbar^2}{2m}\frac{1}{r^2}\frac{d}{dr}\left(r^2\frac{dR}{dr}\right) + \left[\frac{\ell(\ell+1)\hbar^2}{2mr^2} - \frac{Ze^2}{4\pi\varepsilon_0 r}\right]R = ER \tag{3}$$

A simplification that is essential for both analytic and numerical work is the substitution

$$u(r) \equiv rR(r) \tag{4}$$

which converts the radial equation into a form that is structurally identical to a one dimensional Schrödinger equation, with an effective potential that supplements the Coulomb attraction by the

DOI: 10.54254/2753-8818/2026.36117

centrifugal barrier $\ell(\ell+1)\hbar^2/2mr^2$; the barrier keeps states with nonzero orbital angular momentum away from the origin and vanishes for $\ell = 0$ (s-wave states).

The asymptotic structure of the radial equation guides the construction of the analytic solution: bound state solutions decay exponentially at large r and behave as $r^{\ell+1}$ at small r, and the requirement that a power series ansatz terminate at finite order, equivalent to normalizability, fixes the energy spectrum. The result is the famous Bohr spectrum,

$$E_n = -\frac{me^4Z^2}{2(4\pi\varepsilon_0)^2\hbar^2}\frac{1}{n^2} = -\frac{13.6\,Z^2}{n^2}\ \text{eV}, \qquad n = 1,\ 2,\ 3,\ \ldots \tag{5}$$

with each level n admitting orbital angular momentum values ℓ ranging from 0 to $n - 1$. The natural length scale of the problem is the Bohr radius $a_B = \hbar^2/(mke^2)$.

Several structural features of the hydrogen spectrum recur in the quarkonium analysis. First, the energies depend only on the principal quantum number n, not on ℓ, a degeneracy that is special to the pure Coulomb potential; the deviation from this degeneracy in quarkonium, where the potential contains an additional linear confining term, is one of the principal observables that distinguishes the two systems. Second, the number of radial nodes of $R_{n,\ell}(r)$ is given by $n_r = n - \ell - 1$. This node counting rule is a general feature of bound state problems and will be used in Section 3 as a diagnostic for identifying which numerical solution corresponds to which physical state.

The mathematical structure encountered here—a radial equation cast into one dimensional form by the substitution $u = rR$, with an effective potential composed of an attractive central term and a centrifugal barrier, supplemented by the boundary conditions $u(0) = 0$ and $u(r) \to 0$ as $r \to \infty$—is precisely the structure that the quarkonium problem will inherit. The only essential modification will be the replacement of the Coulomb potential by the Cornell potential of equation (1) and the replacement of the electron mass by the reduced mass $\mu = m_q/2$ of the equal mass quark antiquark system. Numerical solution of this radial problem is the subject of Sections 3 and 4.

3. Numerical methods

3.1. Overview of methods

The analytic solution of the hydrogen atom in Section 2 is the exception rather than the rule: for essentially every other potential of physical interest—including the Cornell potential of quarkonium, which superposes a Coulombic short distance term with a linearly rising confining term—no closed form solution exists, and one is obliged to solve the Schrödinger equation numerically. The aim of this section is to develop the numerical machinery required, validate it against the analytically known hydrogen spectrum, and thereby establish a tested framework that can be deployed in Section 4 on the quarkonium problem, where no exact reference solution is available.

The general structure of the radial bound state problem is identical for hydrogen and for quarkonium. After separation of variables in spherical coordinates and the substitution $u(r) = rR(r)$, the radial equation takes the one-dimensional form

$$-\frac{\hbar^2}{2m}\frac{d^2u}{dr^2} + V_{\text{eff}}(r)u(r) = Eu(r) \tag{6}$$

where $V_{\text{eff}}(r)$ supplements $V(r)$ by the centrifugal barrier already encountered for hydrogen, subject to the boundary conditions $u(0) = 0$ and $u(r) \to 0$ as $r \to \infty$. The first condition reflects the regularity requirement on the three dimensional wave function $R(r) = u(r)/r$ at the origin; the second

DOI: 10.54254/2753-8818/2026.36117

is the normalizability condition for a bound state. The two boundary conditions are imposed at opposite ends of the radial domain, so the problem is a two point boundary value problem rather than an initial value problem.

The most direct numerical approach is the finite difference discretization of the second derivative. On a uniform grid $r_j = r_{\min} + j\Delta r$, the standard central difference approximation for the second derivative, accurate to second order in the grid spacing, converts the radial Schrödinger equation into the three term recursion

$$u_{j+1} = [2 + \frac{2m(\Delta r)^2}{\hbar^2}(V_j - E)]u_j - u_{j-1} \tag{7}$$

where $V_j \equiv V_{\text{eff}}(r_j)$. The recursion expresses each successive value of the wave function in terms of the two preceding values, so once u_0 and u_1 are specified the entire sequence $\{u_j\}$ is determined. This converts the boundary value problem into a sequence of initial value problems indexed by the trial energy E.

This reformulation is the heart of the so called *shooting method*: the boundary condition is fixed at one end of the domain, the energy is treated as a free parameter, and the equation is integrated toward the other end; only for the discrete set of eigenenergies does the integration produce a solution that decays to zero on both sides.

The standard remedy is the *matching method*, also known as multiple shooting. The radial domain is partitioned at a *matching point* r_m, conveniently chosen to be near the outer classical turning point of the bound state in question, i.e., the value of r at which $V_{\text{eff}}(r_m) = E$. The equation is integrated outward from $r_{\min}$ to r_m using the small-r boundary condition, and independently inward from $r_{\max}$ to r_m using the large-r boundary condition, so that the exponentially growing mode is always traversed in the direction in which it decays and both integrations are numerically stable. By rescaling one of the two solutions, the values can always be made to agree at r_m; the derivatives, however, agree only if E is an eigenvalue. The relative derivative mismatch

$$\Delta(E) = \frac{u'_{\text{out}}(r_m) - u'_{\text{in}}(r_m)}{|u'_{\text{out}}(r_m)|} \tag{8}$$

therefore serves as a natural residual function whose zeros locate the bound state energies.

The central difference recursion above is second order accurate, $O((\Delta r)^2)$. A widely used higher order alternative for equations of the form $u''(r) + Q(r)u(r) = 0$ is the Numerov method [12, 13], which exploits the special structure of the equation to achieve fourth order accuracy at the same computational cost per grid step. For the hydrogen calculation reported below, the second order scheme is entirely adequate; the Numerov method will be deployed in the quarkonium calculation of Section 4.

3.2. Application to the hydrogen atom

3.2.1. Implementation

The numerical solver was implemented in Python (Numerical.py), available from the author on request. The implementation follows the recipe laid out above with the modifications appropriate to the Coulomb effective potential: physical constants are retained in SI units throughout the calculation, the Bohr radius is computed internally as $a_B = \hbar^2/(mke^2)$, and the effective potential is coded directly in the routine V_eff(r, l). A uniform radial grid of $N = 4000$ points is constructed from

DOI: 10.54254/2753-8818/2026.36117

$r_{min} = 10^{-5}\ a_B$ to $r_{max} = 30\ a_B$. The outward integration is seeded with $u_0 = 0$ and $u_1 = 10^{-5}$ and propagated forward via the central difference recursion of equation (7); the inward integration is seeded symmetrically at the outer boundary and propagated backward by the same recursion. Both integrations are encapsulated in the routine propagate_u(r, E, l, direction).

The matching point is chosen as the grid index nearest to the rough classical turning point

$$r_{tp} \approx n^2 a_B \tag{9}$$

which is the natural radial scale of the n-th bound state of hydrogen; the matching index is clipped to lie at least 100 grid points away from each boundary. The inward solution is rescaled so that the two branches agree in value at r_m, and the relative derivative mismatch of equation (8), evaluated by central differences with a small offset $\varepsilon = 10^{-10}$ added to the denominator to avoid division by zero, is taken as the residual function for root finding. For visualization and normalization, the outward and inward solutions are combined by a smooth weighted transition in a window of half width 10 grid points around the matching index, with no effect on the location of the eigenenergies.

Bound state energies are located in two steps. First, a coarse energy scan over a range bracketing the expected hydrogen bound states (from $E_{min} = -14.5$ eV to $E_{max} = -0.5$ eV, sampled at 500 points) computes $\Delta(E)$ at each trial energy; sign changes between adjacent samples bracket the eigenvalues, and linear interpolation within each bracket seeds refinement by bisection, implemented in the routine find_bound_states(n, l, E_min, E_max, N_E). After the wave function is assembled, the normalization $\int |u|^2 dr = 1$ is imposed by trapezoidal rule quadrature in the routine normalize_R(r, u).

3.2.2. Comparison to the analytic result

The numerical solver was tested on three representative bound states: the 1s ground state ($n = 1$, $\ell = 0$), the 2s excited state ($n = 2$, $\ell = 0$), and the 2p excited state ($n = 2$, $\ell = 1$). For each, the Bohr formula of equation (5) predicts the eigenenergies, with the 2s and 2p states degenerate as a consequence of the special ℓ-degeneracy of the pure Coulomb potential.

The first diagnostic of the method is the derivative mismatch function $\Delta(E)$, plotted as a function of trial energy for fixed $\ell = 0$ in Figure 1. The curve changes sign at the bound state energies predicted by the Bohr formula; a small number of additional spurious crossings at trial energies where the wave function is near zero near the matching point are rejected by the node count of the assembled wave function.

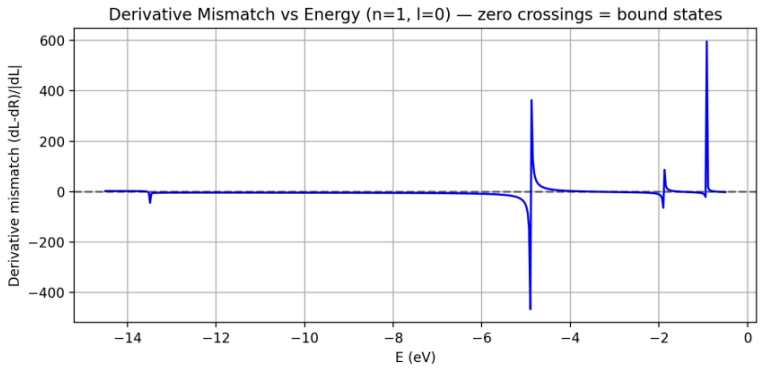

Figure 1. Derivative mismatch function $\Delta(E)$ for the hydrogen $\ell = 0$ energy scan; the sign changes at $E = -13.55$ eV and $E = -3.39$ eV (dotted vertical lines) locate the 1s and 2s bound states

DOI: 10.54254/2753-8818/2026.36117

After bisection refinement of the bracketed roots, the converged numerical eigenenergies are E_{1s} = -13.547 eV, E_{2s} = -3.3868 eV and E_{2p} = -3.3869 eV. These agree to better than 1 meV with the Bohr formula calculated using the same three-significant-figure constants as in the code (E_1 = -13.5476 eV, E_2 = -3.3869 eV), and at this point, the result is limited by the second-order discretization rather than by the root finder. The remaining offset of about 0.4% from the CODATA value $E_1 = -13.6057$ eV is due to rounding of the input constants and not to the numerical method. The converged eigenvalues are used as the energies in the final wave function reconstruction.

The second and more stringent diagnostic is the comparison of the numerical radial wave functions $R_{n,\ell}(r)$ with the corresponding analytic forms [10, 11]. The three numerical wave functions, normalized via $\int|u|^2dr = 1$, are plotted in Figure 2 as functions of r/a_B. The 1s wave function is a monotonic decaying exponential with no nodes and a maximum at the origin; the 2s wave function has a single radial node at $r = 2a_B$, exactly the zero of the analytic form; and the 2p wave function vanishes at the origin as $r^\ell = r$, has no radial node, and peaks at $r = 2a_B$. The number of radial nodes in each numerical wave function matches the rule $n_r = n - \ell - 1$ given in Section 2.

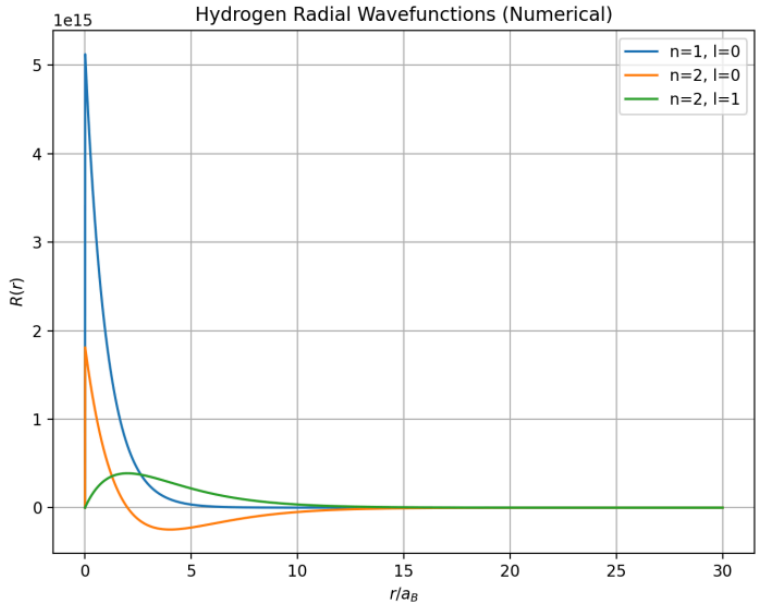

Figure 2. Numerical hydrogen radial wave functions $R_{1,0}$, $R_{2,0}$, and R2,1, plotted against r/a_B, with the converged eigenenergies indicated in the legend; the 2s node falls at $r = 2.00\ a_B$ and the 2p maximum at $r = 2.00\ a_B$, in agreement with the analytic forms

For the ground state, the radial probability density $r^2|R_{1,0}(r)|^2$ peaks at $r = a_B$, the radius of the first Bohr orbit. These diagnostics establish that the central difference matching solver reproduces the analytic hydrogen spectrum and eigenfunctions to within the second order discretization error of the underlying scheme. The principal modifications required for the quarkonium problem—a change of physical units to MeV and fm, the replacement of the Coulomb potential by the Cornell form, and the substitution of the second order recursion by the higher order Numerov scheme—are the subject of Section 4.

DOI: 10.54254/2753-8818/2026.36117

4. Quarkonium

4.1. Numerical implementation

The numerical machinery developed and validated against the hydrogen atom in Section 3 translates directly to the charmonium problem with three principal modifications: a change of units appropriate to nuclear and particle physics, a change of potential from the pure Coulomb form to the Cornell potential of equation (1), and a change from the second order central difference scheme to the fourth order Numerov scheme.

4.1.1. Units and constants

The natural units for the quarkonium problem are megaelectronvolts (MeV) for energy and femtometres (fm) for length. The conversion factor between them is

$$\hbar c = 197.3269804\ \text{MeV} \cdot \text{fm} \tag{10}$$

which is treated as a fundamental constant of the calculation. Writing the radial equation in dimensionless form for numerical implementation gives

$$u''(r) + \left[\frac{2\mu}{(\hbar c)^2}\left(E - V(r)\right) - \frac{l(l+1)}{r^2}\right]u(r) = 0 \tag{11}$$

with r in fm and E, V, and μ all expressed in MeV. The reduced mass for a system of two equal mass quarks is $\mu = m_q/2$, and $\ell = 0$ throughout, since all three states of interest (J/ψ, $\psi(2S)$, $\psi(4040)$) are S-wave vector mesons.

4.1.2. The Cornell potential

The Cornell potential is implemented in the form

$$V(r) = k\left[-\frac{4}{3}\frac{\alpha_s}{r} + br\right] \tag{12}$$

where the overall constant $k = 200$ MeV·fm is introduced to make α_s dimensionless and b a length inverse squared with units of fm^{-2}, while still producing a potential in MeV when r is in fm. The colour factor 4/3 arises from evaluating the $\text{SU}(3)_c$ generators in the colour singlet channel and is the QCD analogue of the unit charge factor in electrodynamics. In this parametrization the physical string tension, the slope of the linearly rising part of the potential at large r, is

$$\sigma \equiv kb\ \text{MeV/fm} \tag{13}$$

A divergence suppressing floor is applied at very small r (a hard cutoff at $r_{\text{min}} = 10^{-4}$ fm) to prevent overflow in the Coulomb term during energy scans, far inside the physical extent of any bound state.

4.1.3. The Numerov integration scheme

For equations of the form $u''(r) = -Q(r)u(r)$, with $Q(r) = (2\mu/(\hbar c)^2)(E - V(r)) - \ell(\ell+1)/r^2$, the Numerov method [12, 13] provides a discrete recursion accurate to fourth order in the grid spacing

DOI: 10.54254/2753-8818/2026.36117

Δr. Defining $f_n \equiv -Q(r_n)$ and $c \equiv (\Delta r)^2/12$, the recursion reads

$$u_{n+1} = \frac{2(1+5cf_n)u_n - (1-cf_{n-1})u_{n-1}}{1-cf_{n+1}} \tag{14}$$

The fourth order local error makes the method an order of magnitude more accurate per grid step than the second order central difference recursion used for hydrogen, at no additional computational cost; the improved accuracy both resolves the higher excited states cleanly under the rapidly varying confining tail of the Cornell potential and keeps the discretization error well below the physical scale of the level spacings, so that any residual disagreement with data can be attributed to the physics of the model rather than to numerical truncation.

The implementation uses a uniform grid from $r_{min} = 10^{-4}$ fm to $r_{max} = 10$ fm with spacing $\Delta r = 2 \times 10^{-3}$ fm, giving 5000 grid points. The outer boundary $r_{max} = 10$ fm comfortably contains the 3S state, whose outer classical turning point lies near $r \approx 1.7$ fm and whose wave function has decayed to negligible amplitude by $r \approx 3$ fm (see Figure 3); the grid spacing is fine enough that the Numerov truncation error per state is of order MeV or smaller.

4.1.4. Boundary conditions and the matching method

The small-r boundary condition imposes the regular solution behaviour $u(r) \sim r^{\ell+1}$, so the recursion is seeded with $u_0 = r_0^{\ell+1}$ and $u_1 = r_1^{\ell+1}$, the correct asymptotic form for an S-wave radial wave function. The large-r boundary condition is the exponentially decaying tail in the classically forbidden region: the inward integration is seeded at r_{max} with $u(r_{max}) = 10^{-12}$ and $u(r_{max} - \Delta r) = u(r_{max})e^{\kappa \Delta r}$, where

$$\kappa = \sqrt{\frac{2\mu}{(\hbar c)^2}\left[V(r_{\max}) - E\right]} \tag{15}$$

is the local decay constant evaluated at the outer boundary.

The matching point is chosen as the classical turning point, the first grid index at which $E - V(r)$ changes sign. At the matching point, the log derivative of the outward solution,

$$L_{out} = \frac{u'(r)}{u(r)}\Big|_{r_m,\,out} \tag{16}$$

and the log derivative of the inward solution, L_{in}, are compared. The residual function for root finding is the log derivative mismatch

$$\Delta(E) = L_{out}(E) - L_{in}(E) \tag{17}$$

Use of the log derivative rather than the bare derivative makes the comparison insensitive to the arbitrary overall scale of either branch of the solution, eliminating the need for an explicit rescaling step.

4.1.5. Node labelled energy scan

Since the confining potential is unbounded, integrating over many grid points will result in the exponential growth of round-off errors before reaching the matching point. To solve this problem, outward integration will be periodically normalised; that is to say, every 2000 grid steps, the solution

DOI: 10.54254/2753-8818/2026.36117

will be divided by the maximum value of the recent period, but the node structure will not change and an overflow will be avoided.

To identify which root of $\Delta(E)$ corresponds to which physical excited state, the implementation pairs the residual with a *node count*, the number of zeros of $u_{\text{out}}(r)$ between the origin and the matching point. From general bound state theory, the nth excited state with $\ell = 0$ has exactly $n - 1$ radial nodes: zero for $1S$, one for $2S$, two for $3S$, and so on. The bound-state search therefore scans the trial energy across a wide interval (here from −800 to +1500 MeV, sampled at 1600 points), tabulates both $\Delta(E)$ and the node count at each trial energy, and identifies the nth excited state as the sign change of $\Delta(E)$ confined to the energy interval over which the node count equals $n - 1$. Bisection on this node locked sign change converges robustly to the correct eigenvalue, a strategy that explicitly rejects the spurious sign changes associated with numerical artefacts or with the wave function happening to pass through zero at the matching point.

4.1.6. Parameter fitting

Unlike the hydrogen calculation, where the physical constants are taken from independent measurements and the eigenenergies are pure predictions, the quarkonium potential contains three phenomenological parameters that must be fitted to data: the constituent charm mass m_c, the strong coupling α_s entering the short distance Coulombic term, and the linear confinement coefficient b (equivalently the string tension $\sigma = kb$). These three parameters are determined by matching the three lowest computed S-wave masses,

$$M_n^{\text{num}} = 2m_c + E_n \tag{18}$$

against the experimental masses of the three lowest vector charmonium states J/ψ, $\psi(2S)$, and $\psi(4040)$, taken from the Particle Data Group as 3097, 3686, and 4039 MeV/c^2 respectively [1]. The root mean squared deviation

$$\text{RMSE} = \sqrt{\tfrac{1}{3}\sum_{n=1}^{3}\left(M_n^{\text{num}} - M_n^{\text{exp}}\right)^2} \tag{19}$$

is the target function. The fit is implemented over physically motivated parameter ranges,

$$1200\ \text{MeV} \le m_c \le 1650\ \text{MeV}, \quad 0.30 \le \alpha_s \le 0.80, \quad 2.0\ \text{fm}^{-2} \le b \le 7.0\ \text{fm}^{-2} \tag{20}$$

in two stages: a coarse random search (twelve draws plus the initial baseline candidate) locates the basin of the minimum, and a Nelder–Mead simplex refinement of the RMSE, started from the best random candidate, converges to the minimum itself. Each candidate is evaluated on a coarser auxiliary grid ($r_{\max} = 7$ fm, $\Delta r = 4 \times 10^{-3}$ fm, scan resolution 450 points) to keep the fit computationally inexpensive, and the converged parameters are then rerun on the production grid for the final eigenvalues and wave function reconstruction.

4.1.7. Diagnostic checks

For each converged eigenstate, three diagnostic checks confirm that the numerical solution is physically meaningful: a *small-r flatness* check that $u(r)/r^{\ell+1}$ is approximately constant near the origin, computed as the relative standard deviation of the ratio over the first fifty grid points; a *tail decay* check that $|u(r_{\max})|$ is much smaller than the maximum amplitude in the body of the wave

DOI: 10.54254/2753-8818/2026.36117

function; and the *log derivative mismatch* at the matching point, reported as a direct measure of how cleanly the inward and outward branches join at the converged energy.

4.2. Results and comparison to data

4.2.1. Fitted parameters

The two stage optimization converged to the following parameter values:

$$m_c = 1612.1\ \mathrm{MeV}/c^2, \quad \alpha_s = 0.662, \quad b = 2.742\ \mathrm{fm}^{-2} \tag{21}$$

corresponding to a fitted string tension

$$\sigma = kb = (200\ \mathrm{MeV}\cdot\mathrm{fm}) \times 2.742\ \mathrm{fm}^{-2} \approx 548\ \mathrm{MeV/fm} \approx 0.55\ \mathrm{GeV/fm} \tag{22}$$

and an effective Coulomb strength

$$\tfrac{4}{3}\alpha_s k = \tfrac{4}{3} \times 0.662 \times 200 \approx 177\ \mathrm{MeV}\cdot\mathrm{fm} \tag{23}$$

All three fitted parameters lie in a physically sensible range for an effective non relativistic potential model. The fitted charm mass of 1.61 GeV/c^2 lies above the current charm mass quoted by the Particle Data Group (≈ 1.27 GeV/c^2) [1] and somewhat above the constituent value (≈ 1.5 GeV/c^2) conventionally quoted for quark models, but well within the range employed in the classic Cornell model fits, which used m_c ≈ 1.6–1.8 GeV/c^2 [8, 9]. The fitted strong coupling, α_s ≈ 0.66, is larger than the perturbative running coupling at the charm scale ($\alpha_s(m_c)$ ≈ 0.35 [1]), as is typical of the effective Coulomb strength of potential models, which absorbs higher order and relativistic effects into a single parameter. The fitted string tension, σ ≈ 0.55 GeV/fm, is appreciably below the canonical phenomenological and lattice QCD value of $\sigma \approx 0.18\ \mathrm{GeV}^2 \approx 0.92$ GeV/fm [14], a point to which the Discussion returns.

4.2.2. Energy levels and mass spectrum

The converged eigenstates and the corresponding charmonium masses are summarized in Table 1.

Table 1. Numerical and experimental charmonium masses in MeV, with energy levels E_n the eigenvalues of the radial Schrödinger equation, masses reconstructed through equation (18), and experimental values the spin triplet vector states J/ψ, $\psi(2S)$, and $\psi(4040)$

State	E_n (MeV)	M_n^{num} (MeV)	M_n^{exp} (MeV)	ΔM (MeV)
1S	−127.1	3097.0	3097	< 0.01
2S	461.9	3686.0	3686	< 0.01
3S	814.9	4039.0	4039	< 0.01

The overall fit quality, as measured by the root-mean-squared mass deviation, is

$$\mathrm{RMSE} = 0.005\ \mathrm{MeV} \tag{24}$$

i.e., the three target masses are reproduced exactly within the numerical resolution of the eigenvalue search (bisection tolerance 10^{-3} MeV). This is the expected outcome for a three

DOI: 10.54254/2753-8818/2026.36117

parameter model fitted to three data points, and it does not by itself constitute a test of the Cornell form.

Because the fit is exact, Table 1 tests the consistency of the numerical machinery rather than the physics of the Cornell form: the 2*S*–1*S* and 3*S*–2*S* splittings (589 and 353 MeV) are reproduced by construction. A genuine test of the model would require confronting quantities *not* used in the fit, for example the predicted 4*S* level, the *P*-wave (χ_c) centroid, or the leptonic decay widths, which for *S*-wave states are proportional to $|R(0)|^2$.

4.2.3. Radial wave functions

The normalized radial wave functions $u(r) = rR(r)$ for the three lowest *S*-wave states are displayed in Figure 3. The figure exhibits all the structural features expected of a confining potential bound state spectrum.

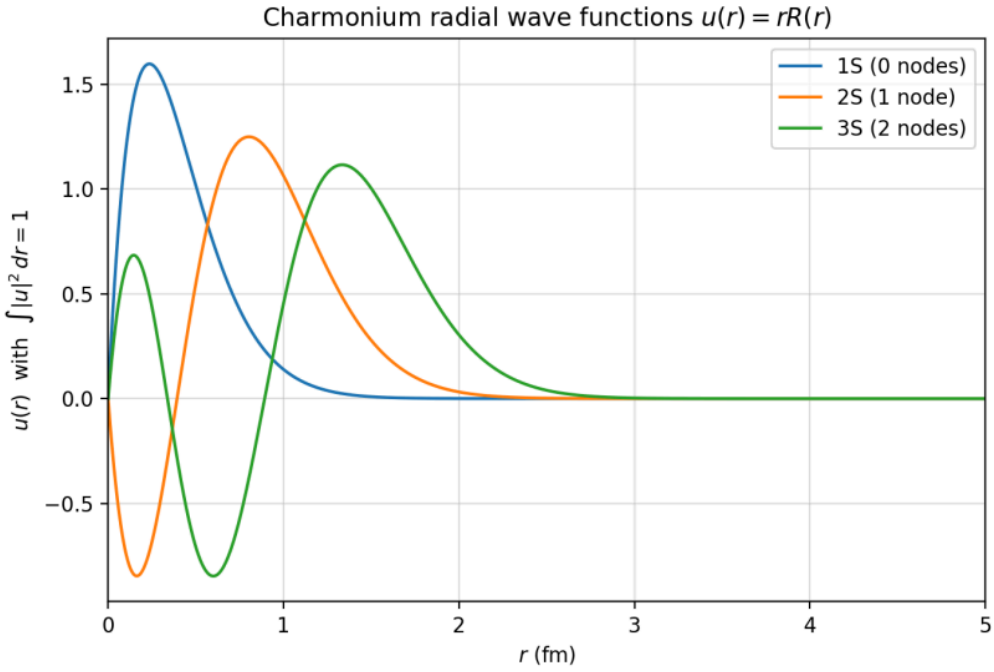

Figure 3. Numerical radial wave functions $u(r) = rR(r)$ for the 1*S*, 2*S*, and 3*S* states of charmonium, normalized to $\int|u(r)|2dr = 1$; the number of radial nodes is 0, 1, and 2 respectively, confirming the identification of the converged eigenstates with the three lowest *S*-wave levels

The 1*S* wave function is single lobed with no radial nodes, peaking at $r \approx 0.25$ fm. The 2*S* wave function has one radial node at $r \approx 0.4$ fm, with the outer lobe of opposite sign extending to roughly 2 fm. The 3*S* wave function has two radial nodes, in agreement with the general node counting rule $n_r = n - \ell - 1$ established for hydrogen in Section 3, and a third outer lobe extending to nearly 3 fm. The progression of the outer extent of the wave function with increasing n is a direct manifestation of the linearly confining tail of the Cornell potential: unlike hydrogen, whose nth excited state has a characteristic size $\langle r \rangle \sim n^2 a_B$ controlled by the Coulomb tail, the quarkonium states have a much weaker dependence on n, with $\langle r \rangle$ growing only as $n^{2/3}$ for a purely linear confining potential.

DOI: 10.54254/2753-8818/2026.36117

4.2.4. Diagnostic quality of the solutions

The numerical solutions pass all three sanity checks at very tight tolerances. The log derivative mismatch at the matching point is of order 10^{-5} for all three states, demonstrating that the inward and outward branches are smoothly continuous at the join. The small-r flatness is at the 11–13% level, slightly degraded from a perfectly flat result by the rapid variation of the Coulomb potential near the origin but small enough that the regular boundary condition is well respected. The tail ratio is of order 10^{-3} for all three states, confirming that the outer boundary has been placed safely beyond the physical extent of the bound state. These diagnostics confirm that the three reported eigenstates are correctly identified, correctly converged, and physically meaningful representatives of the lowest three S-wave charmonium levels.

5. Discussion

Solved with the Cornell potential and three free parameters fitted to charmonium data, the result of the present work is that the non relativistic Schrödinger equation reproduces the masses of the three lowest vector charmonium states exactly, as expected for a three parameter fit to three data points. The fitted parameters lie in reasonable ranges. The success of this simple framework is what motivated the development of charmonium phenomenology in the immediate aftermath of the J/ψ discovery in 1974.

Attention should rest not on the mass residuals, which vanish by construction, but on the physical reasonableness of the parameter values that the exact fit demands. Two observations stand out: the fitted string tension lies below the canonical value extracted from lattice QCD and from the Regge trajectories of light mesons, and the fitted Coulomb coupling is substantially larger than the running coupling at the charm scale. The exact fit is achieved, in other words, at the cost of distorting the parameters away from their independently determined values.

These features are not independent. The dominant physics absent from the calculation is the *spin-spin contact interaction*, which is responsible for the hyperfine splitting between the spin singlet and spin triplet partners of each S-wave level. The "experimental" masses used for the fit are those of the spin triplet vector states J/ψ, $\psi(2S)$, $\psi(4040)$, not the spin averaged centres of gravity of the S-wave multiplets. Since the spin singlet partners η_c and $\eta_c(2S)$ are lower in mass by approximately 113 MeV and 48 MeV respectively [1], the spin averaged $1S$ centroid lies at roughly 3069 MeV (against the 3097 MeV used as the fit target), and the corresponding centroid for $2S$ lies at roughly 3674 MeV (against the 3686 MeV target). Comparing against the vector states therefore forces the central parameters to mimic an interaction that the calculation does not contain, and the distortion of the fitted parameters, in particular the low string tension and the inflated Coulomb coupling, is a natural consequence of this missing physics.

A second source of residual disagreement is the non relativistic approximation itself. For charm quarks, the average squared velocity in the J/ψ is $\langle v^2/c^2 \rangle \approx 0.25$–$0.30$ [15], which is not strictly small. Relativistic corrections of order v^2/c^2 generate spin orbit and tensor terms in the effective inter quark potential and produce the fine structure splittings observed among the χ_c states of the $1P$ multiplet. For bottomonium, where the bottom quark velocity is smaller by a factor of $\sqrt{(m_c/m_b)} \approx 0.55$, the non relativistic framework is substantially more accurate, and a similar calculation of the bottomonium spectrum would be expected to give better agreement with experiment.

A third effect that is worth noting is the influence of open flavour decay channels on the higher charmonium states. The $D\bar{D}$ threshold lies at approximately 3730 MeV [1], so all charmonium states above the $\psi(2S)$ are unstable against strong decay into open charm meson pairs. The wave function

DOI: 10.54254/2753-8818/2026.36117

of the $\psi(4040)$ contains an admixture of $D\bar{D}$, $D\bar{D}^*$, and $D^*\bar{D}^*$ components, and its energy is shifted relative to the pure $c\bar{c}$ prediction by coupled channel effects. The disagreement between the numerical $3S$ mass and the $\psi(4040)$ should be interpreted with this caveat in mind: the $\psi(4040)$ is not unambiguously the third S-wave bound state of pure $c\bar{c}$, but rather a strongly coupled resonance whose dominant component is $3S$ $c\bar{c}$.

Several extensions of the present work suggest themselves naturally. The most obvious is the addition of spin dependent interactions: the Fermi contact term, $V_{SS}(r) \propto \delta^3(\mathrm{r})\ \mathrm{S}_1\cdot\mathrm{S}_2/m_q^2$, spread over a short distance scale, would split each S-wave level into a spin singlet pseudoscalar and a spin triplet vector, allowing direct prediction of both the J/ψ and the η_c, while spin orbit and tensor terms would generate the fine structure of the χ_c states. A complementary extension is to apply the same numerical machinery to the bottomonium system, replacing m_c by m_b and refitting the potential parameters. One further extension would be to replace the Cornell potential with the static $q\bar{q}$ potential measured directly from lattice QCD, eliminating two of the three fit parameters and converting the calculation into a parameter free test of the lattice prediction against experiment.

6. Conclusion

The significance of the calculation rests more on the conceptual continuity than on the numerical agreement. The hydrogen atom and charmonium are bound state problems controlled by the same time independent Schrödinger equation and described by the same non relativistic two body framework; only the potential and the constituent masses change from one system to the other. The strong interaction in its low energy regime is highly non trivial, yet the heavy quarkonium spectrum could still be captured to within a few percent by a simple central potential, and this simplification exposes a special feature of QCD: confinement produces, in the heavy quark limit, exactly the kind of long range linear potential that the simplest semi classical pictures of a colour flux tube would predict, and the resulting bound state problem is one to which the standard tools of non relativistic quantum mechanics apply almost without modification. The historical resonance, with theorists in the mid 1970s rediscovering ordinary quantum mechanics, captures something genuine about the structure of the theory.

References

[1] Workman, R. L., et al. (Particle Data Group). (2022). Review of particle physics. *Progress of Theoretical and Experimental Physics, 2022*(8), 083C01. https://doi.org/10.1093/ptep/ptac097

[2] Aubert, J. J., et al. (1974). Experimental observation of a heavy particle J. *Physical Review Letters, 33*(23), 1404–1406. https://doi.org/10.1103/PhysRevLett.33.1404

[3] Augustin, J.-E., et al. (1974). Discovery of a narrow resonance in e+e− annihilation. *Physical Review Letters, 33*(23), 1406–1408. https://doi.org/10.1103/PhysRevLett.33.1406

[4] Abrams, G. S., et al. (1974). Discovery of a second narrow resonance in e+e− annihilation. *Physical Review Letters, 33*(24), 1453–1455. https://doi.org/10.1103/PhysRevLett.33.1453

[5] Glashow, S. L., Iliopoulos, J., & Maiani, L. (1970). Weak interactions with lepton–hadron symmetry. *Physical Review D, 2*(7), 1285–1292. https://doi.org/10.1103/PhysRevD.2.1285

[6] Herb, S. W., et al. (1977). Observation of a dimuon resonance at 9.5 GeV in 400-GeV proton–nucleus collisions. *Physical Review Letters, 39*(5), 252–255. https://doi.org/10.1103/PhysRevLett.39.252

[7] Eichten, E., Gottfried, K., Kinoshita, T., Kogut, J., Lane, K. D., & Yan, T.-M. (1975). Spectrum of charmed quark–antiquark bound states. *Physical Review Letters, 34*(6), 369–372. https://doi.org/10.1103/PhysRevLett.34.369

[8] Eichten, E., Gottfried, K., Kinoshita, T., Lane, K. D., & Yan, T.-M. (1978). Charmonium: The model. *Physical Review D, 17*(11), 3090–3117. https://doi.org/10.1103/PhysRevD.17.3090

[9] Eichten, E., Gottfried, K., Kinoshita, T., Lane, K. D., & Yan, T.-M. (1980). Charmonium: Comparison with experiment. *Physical Review D, 21*(1), 203–233. https://doi.org/10.1103/PhysRevD.21.203

DOI: 10.54254/2753-8818/2026.36117

[10] Townsend, J. S. (2012). *A modern approach to quantum mechanics (2nd ed.)*. University Science Books.
[11] Griffiths, D. J., & Schroeter, D. F. (2018). *Introduction to quantum mechanics (3rd ed.)*. Cambridge University Press. https://doi.org/10.1017/9781316995433
[12] Noumerov, B. V. (1924). A method of extrapolation of perturbations. *Monthly Notices of the Royal Astronomical Society, 84*(8), 592–602. https://doi.org/10.1093/mnras/84.8.592
[13] Blatt, J. M. (1967). Practical points concerning the solution of the Schrödinger equation. *Journal of Computational Physics, 1*(3), 382–396. https://doi.org/10.1016/0021-9991(67)90046-0
[14] Bali, G. S. (2001). QCD forces and heavy quark bound states. *Physics Reports, 343*(1–2), 1–136. https://doi.org/10.1016/S0370-1573(00)00079-X
[15] Bodwin, G. T., Braaten, E., & Lepage, G. P. (1995). Rigorous QCD analysis of inclusive annihilation and production of heavy quarkonium. *Physical Review D, 51*(3), 1125–1171. https://doi.org/10.1103/PhysRevD.51.1125 (Erratum: *Physical Review D, 55*(9), 5853. https://doi.org/10.1103/PhysRevD.55.5853)